Research Article ISSN 2639-846X

Anesthesia & Pain Research

Changes in Electroencephalogram (EEG) After Foot Stimulation with Embedded Haptic Vibrotactile Trigger Technology: Neuromatrix and Pain Modulation Considerations

Baldeep S. Dhaliwal[1], John Haddad[2], Mark Debrincat[3] and Peter Hurwitz[4*]

[1]*Toronto, Ontario, Canada.*

[2]*American University, Beirut, Lebanon.*

[3]*Castle Rock, Colorado.*

[4]*Clarity Science LLC, Narragansett, Rhode Island, USA.*

[*]Correspondence:

Peter Hurwitz, Clarity Science LLC, 750 Boston Neck Road, Suite 11, Narragansett, RI 02882, USA, Tel: +1917 757 0521.

Received: 01 Nov 2022; **Accepted:** 12 Dec 2022; **Published:** 16 Dec 2022

Citation: Dhaliwal BS, Haddad J, Debrincat M, et al. Changes in Electroencephalogram (EEG) After Foot Stimulation with Embedded Haptic Vibrotactile Trigger Technology: Neuromatrix and Pain Modulation Considerations. Anesth Pain Res. 2022; 6(2): 1-11.

ABSTRACT

Background: *Globally, pain and pain-related diseases are the leading causes of disability and disease burden. In the United States, pain is the most common reason patients consult primary care providers. An estimated 100 million people live with chronic or recurrent pain. Existing pharmacological treatments for pain include anti-inflammatory agents, opioids, and other oral and topical analgesics. Many of these have been associated with troublesome and potentially harmful adverse effects. Understanding the complex pain neuromatrix may help in identifying alternative, non-invasive strategies and treatment approaches to address pain severity, interference, and improve patient outcomes.*

The neuromatrix of pain is a network of neuronal pathways and circuits responding to sensory (nociceptive) stimulation. Research has suggested that the output patterns of the body-self neuromatrix are responsible for causing or triggering perceptual, homeostatic, and behavioral programs following traumatic injury, other pathology, or chronic stress. As such, pain can be considered a product of the output of a widely distributed neural network within the brain instead of a sequential result of sensory inputs triggered by injury, inflammation, or other pathology. For over a century, the Brodmann Areas remain the most widely known and frequently cited cytoarchitectural organization of the human cortex. Certain Brodmann areas of the brain have been associated with the current understanding of the neuromatrix of pain. The areas expands well beyond the thalamus and anterior cingulate, and primary (S1) and secondary (S2) somatosensory cortices to include the midbrain region of the periaqueductal gray (PAG) and the lenticular complex as well as the insula, orbitofrontal (Brodmann's area [BA] 11, 47), prefrontal (BA 9, 10, 44-46), motor (BA 6, Supplementary motor area, and M1), inferior parietal (BA 39, 40), and anterior cingulate (BA 24, 25) cortices (ACCs). Treatments that are non-invasive and non-pharmacological and target both central and peripheral nociceptive mechanisms that are identified as having an impact on the Brodmann areas associated with the neuromatrix of pain may potentially be considered a beneficial pain management option for patients.

Haptic vibrotactile trigger technology targets the nociceptive pathways and is theorized to disrupt the neuromatrix of pain. The technology has been incorporated into non-pharmacological patches and other non-invasive routes of delivery such as apparel (socks), braces, wristbands, and compression sleeves.

The purpose of this minimal risk study was to compare electroencephalogram (EEG) patterns in areas of the brain that have been associated with the neuromatrix for pain in subjects wearing socks that were embedded with haptic vibrotactile trigger technology with those patients that wore socks that were not embedded with the technology.

Methods: *This IRB-approved study compared electroencephalogram (EEG) patterns in subjects wearing cloth socks embedded with haptic vibrotactile trigger technology (Superneuro VTT Enhanced Socks (Srysty Holding Co., Toronto, Canada) with those patients that wore cloth socks that were not embedded with the technology. Baseline EEG data from 19 scalp locations were recorded in sixty (60) adult subjects (36 females and 24 males) ranging from ages 14 to 83 wearing standard store-purchased cloth socks on their feet. The subject's standard socks were then removed and replaced with the Superneuro VTT enhanced socks on the subject's feet. A second EEG recording was then obtained. Both eyes-closed and eyes-open data were recorded.*

Results: *The results showed statistically significant t-test differences ($P < .01$) in 59 out of 60 subjects in absolute power and 60 out of 60 subjects showed statistically significant differences in coherence and phase difference. The largest differences were in the alpha1 and beta2 frequency bands and especially in central scalp locations. Paired t-tests of LORETA current source densities between socks on and socks off demonstrated statistically significant differences in 60 out of 60 subjects. The largest effects of Superneuro VTT enhanced socks on were on the medial bank of the somatosensory cortex as well as in the left frontal lobes in the theta and alpha frequency.*

Conclusions: *Study results indicate that foot stimulation with embedded haptic vibrotactile trigger technology showed significant modulation in the Brodmann areas that have been shown to be associated with the neuromatrix for pain in the human brain. Further research is suggested to evaluate if this technology has a positive impact on pain severity, pain interference, and quality of life and to be considered as a potentially beneficial pain management strategy and as part of a multi-modal treatment approach.*

Keywords
Haptic vibrotactile trigger technology, Pain modulation, Neuromatrix of pain, Pain management, Analgesic, Superneuro, VTT.

Introduction
Globally, pain and pain-related diseases are the leading causes of disability and disease burden. In the United States, pain is the most common reason patients consult primary care providers and an estimated 100 million people live with chronic or recurrent pain [1].

Existing treatments for pain include non-pharmacological and pharmacological approaches [2-5]. Some of these treatments can be non-invasive. Increased prescribing of pharmacological treatments, including opioids and non-opioid drugs, such as NSAIDS, have occurred over the last decade [6-8]. Many of these treatments have known side effects, including GI toxicity, bleeding, and the potential for addiction, abuse, and death [9-12]. There has been an effort to identify alternative treatments that are targeted and non-invasive that would be part of a multi-modal approach that would lead to a reduction in dangerous side effects [13]. Guidelines for pain management from several Medical Associations, including the American Academy of Family Physicians (AAFP), the American College of Physicians (ACP), and the American College of Rheumatology (ACR), recommend a multi-modal approach to address pain that includes non-invasive and non-pharmacological therapies as a first line treatment before consideration of other approaches [14,15].

Understanding the mechanisms of pain has led to advancements of new technologies and new routes of delivering these technologies with the objective to decrease side effects and improve patient outcomes. Non-invasive and non-pharmacological approaches have been shown safe and effective for chronic pain patients and have the potential to minimize side effects associated with traditional medication or interventional therapies [16].

Over the past several years, researchers have developed an understanding of the Neuromatrix Theory of Pain (NTP) through a broad base of imaging studies and related theories of how different brain regions interact and sense pain.

Acute pain is a noxious bodily sensation occurring as part of the brain's passive response to tissue damage, the neural mechanisms of which have been well characterized. Not all pain sensations are the result of ongoing physical trauma despite the perception of pain, as in the cases of phantom limb, chronic pain, or emotional pain [17]. Whether acute or chronic, the body's ability to perceive pain is the result of communicating with the peripheral (PNS) and central nervous systems (CNS). Phantom limb and chronic pain states, which may involve aberrant communication between the PNS and CNS, remain poorly understood [18]. One reason for this is that chronic pain perception appears to involve multiple neural pathways in addition to those associated with acute pain [18,19]. These networks involved in the perception of painful sensations, as well as their communication and coordination between the CNS and PNS, are referred to broadly as the "neuromatrix", which is the basis for the NTP [17].

The NTP was first proposed by Ronald Melzack, who hypothesized that networks of neurons communicating in "large loops", or through continuous cyclical processing, connect specific regions of the brain with the PNS during sensory processing [17]. Melzack envisioned 3 distinct looping pathways. One follows a traditional sensory pathway, with neural projections routed through the thalamus. Projections in the second loop follow a path through the brainstem and parts of the limbic system. In the third loop, pathways are routed through different Brodmann Areas (BA), particularly the somatosensory cortex. These proposed loops were meant to explain the cognitive, emotional, and motor modalities through which humans experience sensations, particularly pain [17,20].

The neuromatrix incorporates sensory inputs from the PNS and uses this input to create different output responses. These patterns of sensation and response are encoded in the matrix and called "neurosignatures". These neurosignatures serve a dual purpose: to process and respond to sensory stimuli, and to continuously monitor the state of the body and determine if it is intact. In either case, while the original activities and neural outputs of a neuromatrix are guided by an individual's genetics, this changes over time with different sensory experiences, illness, injury, chronic stress, and other factors [17,18]. In the context of pain, a neurosignature pattern can be elicited by outward noxious stimuli. However, pain-associated neurosignatures can also occur independently of external stimuli, as described above in the case of phantom limb and chronic pain [17].

The NTP posits that these different neurosignatures, and the ways they are generated, are the result of complex neural networks. In other words, the sensation of pain is the result of internal mechanisms [17,20]. Since the publication of Melzack's proposed theory, numerous studies have examined the brain's response to pain harnessing the power of modern imaging techniques like PET and fMRI. The regional brain activation documented in these studies largely aligns with what Melzack proposed [20]. That said, the brain regions found to be activated during painful or noxious stimuli in these reports are encompass more of the brain than Melzack assumed, and it appears that activation of these networks alone are not the source of pain perception [20,21]. An early review probing the functionality of the NTP focused on data from PET and fMRI studies that explored regional differences in brain activation during various noxious stimuli. The general conclusion of the review is that many more brain regions are involved in the processing of pain than originally anticipated [20]. Melzack originally implicated general regions: the thalamus, anterior cingulate, and primary (S1) and secondary (S2) somatosensory cortices [17]. This review noted that findings from the more than 30 included studies largely agreed with the original proposed brain areas. What differed was that the reported brain regions were much more regionally specific and spread across a larger area of the

cortex. In addition to the thalamus, several additional regions of the midbrain were identified, including the insula, lenticular complex, and periaqueductal gray (PAG). Additional cortical regions and associated Brodmann areas (BA) were also noted, including parts of the prefrontal cortex (BA 9, 10, 44-46), orbitofrontal cortex (BA 11,47), motor cortex (BA 6, Supplementary motor area, M1), and the inferior parietal cortex (BA 39, 40). The anterior cingulate was also observed to be more regionalized than previously thought (BA 24, 25) [20]. This collection of findings illustrates a broad cortical response to pain perception.

It was recently discovered that when a somatosensory pattern of stimulation is applied to the metatarsal region of the foot then improved balance and movement coordination often occurred (Dhaliwal, 2018) [22]. As a consequence, the somatosensory pattern of stimulation was woven or molded into socks and worn on one's feet to better facilitate the effects of the somatosensory stimulation of the metatarsal region of the bottom of the feet on the peripheral and central nervous system. The purpose of this study was to explore the effects on the human electroencephalogram (EEG) when subjects place specially designed socks that provide tactile pattern pressure on the metatarsal region of the human foot.

Methods

Study Design

This study was an Institutional Review Board-approved Study aimed at comparing electroencephalogram (EEG) patterns in subjects wearing cloth socks embedded with haptic vibrotactile trigger technology (Superneuro VTT Enhanced Socks (Srysty Holding Co., Toronto, Canada) (see Photos 1 and 2) with those patients that wore cloth socks that were not embedded with the technology. The electroencephalogram (EEG) was recorded from 19 scalp locations from 60 subjects ranging in age from 14 years to 83 years (Females = 36, males = 24). An approximate five-minute baseline EEG was recorded with subjects wearing standard store purchased socks on their feet. The subject's standard socks were removed and the Superneuro VTT Enhanced Socks were placed on the subject's feet and a second EEG recording was obtained. Both eyes-closed and eyes-open conditions were recorded. A FFT auto and cross-spectral power analysis of the surface EEG was conducted from 1 Hz to 50 Hz. The variables were absolute power EEG in 1 Hz increments and coherence and phase differences in 10 frequency bands (delta, theta, alpha1, alpha2, beta1, beta2, beta3 and hibeta). Paired t-tests between the standard socks and Superneuro VTT pattern socks conditions were computed for each subject for all EEG measures as well as group paired t-tests.

The study protocol was approved by an institutional review board and was performed in full accordance with the rules of the Health Insurance Portability and Accountability Act of 1996 (HIPAA) and the principles of the declaration of Helsinki and the international council of Harmonisation/GCP. All patients gave informed and written consent.

Haptic Vibrotactile Trigger Technology Intervention

Photo 1: The Superneuro VTT enhanced sock.

Photo 2: The Superneuro VTT enhanced sock

Study Procedures and Assessments

EEG Recording

The Wearable Sensing DSI-24 dry amplifier system was used to amplify and digitize the EEG recorded from 19 scalp electrodes according to the International 10/20 electrode locations. Approximately 2 to 5 minutes of EEG was recorded in the eyes closed condition and the eyes open condition with no socks on the subject's feet. A second 2-to-5-minute recording in the eyes closed and eye open condition was recorded after placing the Superneuro VTT enhanced socks on each subject's feet.

Power Spectral Analyses

Each EEG record was visually examined and manual deselection of segments containing artifact of any type were deleted from the record. Split-half reliability and test re-test reliability measures of the artifact free data were computed using the Neuroguide software program (NeuroGuide, v2.9.9). Split-half reliability tests were conducted on the edited artifact free EEG segments and records with > 90% reliability were entered into the spectral analyses. A Fast Fourier transform (FFT) auto-spectral and cross-spectral analysis was computed on 2 second epochs thus yielding a 0.5 Hz frequency resolution over the frequency range from 0 to 50 Hz for each epoch. A 75% sliding window method was used to compute the FFT in which successive two-second epochs (i.e., 256 points) were overlapped by 500 millisecond steps (64 points) in order to minimize the effects of the FFT windowing procedure.

Surface EEG Coherence

The cross-spectrum was used to compute EEG coherence and phase differences in ten frequency bands: Delta (1 to 4.0 Hz), theta (4 - 8 Hz), alpha (8 - 12 Hz), beta broad (12 - 25 Hz), beta 1 (12 - 15 Hz), beta 2 (15 - 18 Hz), beta 3 (18 - 25 Hz) and hi-beta (25 - 30 Hz). Coherence is a measure of the consistency of the analytical phase differences over some interval of time, is equivalent to a squared correlation coefficient, and is dependent on the number of degrees of freedom used to estimate the consistency of the phase differences. When the phase difference in successive epochs is constant then coherence = 1 and when phase differences are random then coherence = 0. Coherence is mathematically defined as:

$$\Gamma^2{}_{xy}(f) = \frac{\left(G_{xy}(f)\right)^2}{\left(G_{xx}(f)G_{yy}(f)\right)}$$

where G_{xy} (f) is the cross-power spectral density and G_{xx} (f) and G_{yy} (f) are the respective autopower spectral densities. The computational procedure to obtain coherence involved first computing the power spectra for x and y and then computing the cross-spectra. Since complex analyses are involved, this produced the average cospectrum ('r' for real) and quadspectrum ('q' for imaginary). Then coherence was computed as:

$$\Gamma^2_{xy}(f) = \frac{\sum_N \left[r_{xy} + q_{xy}\right]^2}{\sum_N G_{xx} G_{yy}}$$

LORETA Current Density

$J = T \bullet S$ LORETA is a distributed EEG inverse solution where the currents at 3- dimensional gray matter voxels J are a linear combination of the signal S recorded at a scalp electrode:

Where T is a minimum norm 3-dimensional matrix of 2,394 gray matter voxels with x, y and z coordinates in a generalized inverse that weights the solution to sources that are synchronous in local volumes or regions using the 3-dimensional Laplacian Operator (Pasqual-Marqui et al., 1994; Pasqual-Marqui, 1999). The T matrix is mathematically defined as:

$T = \{inv(WB'B\ W)\}\ K'\ \{pinv(WB'BW)K'\}$

Where B is the discrete Laplacian Operator and W is a weighting matrix (inv indicates inverse) and pinv(X) is the Moore-Penrouse pseudoinverse of X (Menke, 1984).

The Talairach Atlas coordinates of the Montreal Neurological Institute's MRI average of 305 brains (Lancaster et al., 2000; Pascual-Marqui, 1999) and the linkage to standard anatomical 7mm x 7mm x 7 mm voxels each with a distinct Talairach Atlas Coordinate. Groups of voxels are also defined by the clear anatomical landmarks established by von Brodmann in 1909 and referred to as Brodmann areas. The resultant [ ] å å + G = N xx yy N xy xy xy G G r q f 2 2 ( ) J = T • S T ={inv(WB'BW)} K'{pinv(WB'BW)K'} 6 current source vector at each voxel was computed as the square root of the sum of the squares for the x, y and z source moments for each 0.5Hz frequency band. In order to reduce the number of variables, adjacent frequency 0.5 Hz bins were averaged to produce nine different frequency bands: delta (1-4 Hz); theta (4-7 Hz); alpha1 (8-10 Hz); alpha2 (10-12 Hz); beta1 (12-15 Hz); beta2 (15-18 Hz); beta3 (18-25 Hz) and hi-beta (25-30 Hz) for each of the 2,394 gray matter voxels.

Statistical Analysis

For all variables, descriptive statistics were calculated, including frequencies and percent for categorical variables and means with standard deviation (SD) for continuous variables. The maximum sample size available was used for each statistical analysis. Paired t-tests between the standard socks and Superneuro VTT pattern socks conditions were computed for each subject for all EEG measures as well as group paired t-tests. A two-tailed alpha was set to 0.05 for all statistical comparisons. SPSS v. 27 was used for all analyses.

Results

During EEG readings where the subjects' eyes were open or closed, Superneuro VTT enhanced socks activated 35 out of 86 BA (left and right hemispheres combined) and 48 out of 86 BA (left and right hemispheres combined), respectively. Among BA that were activated by Superneuro VTT enhanced socks in a statistically significant manner, 10 out of 12 overlapped with the review: 9,11, 24, 39, 40, 44- 47. When compared to standard socks, activation in the medial somatosensory cortex, parts of the occipital lobe, and bilateral frontal lobes were statistically higher while wearing Superneuro VTT enhanced socks ($p<0.001$).

Absolute Power Surface EEG

The percent difference between socks on vs socks off from the 19 scalp electrode locations for the ten frequency bands in the eyes closed condition, the differences ranged from 0.04 % difference at 01 in the alpha frequency band to 54.68 % in the delta frequency band in F7.

Table 1 shows the results of the paired t-tests in absolute EEG power between socks off vs socks on in the eyes closed condition. Statistically significant differences were primarily in the delta and theta frequency bands and especially in the left hemisphere in comparison to the right hemisphere.

FFT Absolute Power Group Paired t-Test (P-Value).

Table 1: Paired t-tests in absolute power in the surface EEG in all frequency bands between socks on versus socks off between socks on and socks off in the eyes closed condition.

lntrahemispheric: LEFT

	DELTA	THETA	ALPHA	BETA	HIGH BETA	BETA 1	BETA 2	BETA3
FP1 -LE	0.207	0.107	0.573	0.474	0.426	0.618	0.598	0.312
F3- LE	0.031	0.003	<0.757	0.89	0.826	0.714	0.79	<0.642
C3-LE	0	0.014	0.837	0.993	0.365	0.92	0.606	0.788
P3-LE	0.108	0.031	0.581	0.455	0.521	0.461	0.423	0.225
O1-LE	0.51	0.096	0.77	0.678	0.119	0.642	0.419	0.35
F7 - LE	0.016	0.023	0.407	0.462	0.572	0.205	0.416	o.n5
T3- LE	0.024	0.057	0.549	0.194	0.555	0.223	0.196	0.358
T5- LE	0.015	0.005	0.552	0.689	0.638	0.241	0.276	0.508

lntrahemispheric: RIGHT

	DELTA	THETA	ALPHA	BETA	HIGH BETA	EIETA 1	EIETA 2	EIETA 3
FP2- LE	0.239	o.=	0.607	0.42	0.631	0.555	0.608	0.44
F4- LE	0.336	0.4	0.42	0.56	0.358	0.499	0.57	0.208
C4- LE	0.494	0.29	0.263	0.25	0.565	0.766	0.79	0.213
P4- LE	0.039	0.016	<0.584	0.63	0.873	0.767	0.23	<0.845
O2-LE	0.464	0.678	0.585	0.31	0.168	0.2M	0.735	0.097
FB - LE	0.462	0.594	0.414	0.001	0.439	0.262	0.422	0.26,
T4-LE	0	0	0.079	0.97	0.04	0.021	0.026	0.274
T6-LE	0.287	0.529	0.984	0.03	0.348	0.404	0.801	0.313

lntrahemispheric: CENTER

	DELTA	THETA	ALPHA	BETA	HIGH BETA	EIETA 1	EIETA 2	EIETA 3
Fz- LE	0.187	0.077	0.873	0.764	0.505	0.91	0.889	0.419
Cz- LE	0.435	0.546	0.499	0.428	0.234	0.76	0.997	0.089
Pz- LE	0.458	0.956	0.853	0.77	0.527	0.471	0.55	0.819

The percent difference between socks on vs socks off from the 19 scalp electrode locations for the ten frequency bands in the eye's closed condition was measured. The differences ranged from 0.06 % difference at Cz in the beta frequency band to 62.26 % in the delta frequency band in P4.

Evaluation of the paired t-tests in absolute EEG power between socks off vs socks on in the eyes open condition resulted in statistically significant differences (P< .05) that were present bilaterally with increased power in the lower frequency bands. Statistically significant reduction in absolute power were present in the higher frequency bands in the right hemisphere.

Surface EEG Coherence

Figure 1 shows the results of paired t-tests in the surface EEG coherence measures between socks off vs socks on in the eyes closed condition. Significant differences (P < .05) were present in widespread electrode pairs and in all frequency bands in both the left and right hemispheres. The socks on condition generally resulted in reduced coherence with the exception of the interhemispheric temporal lobes (T3-T4) in the delta frequency band.

Figure 2 shows the results of paired t-tests in the surface EEG coherence measures between socks off vs socks on in the eyes open condition. Significant differences (P < .05) were present in widespread electrode pairs and in all frequency bands in both the left and right hemispheres. The socks on condition consistently resulted in reduced coherence.

LORETA Current Density

Table 2 shows the results of paired t-tests in LORETA current density in the eyes closed condition between socks off and socks on. The effects appeared to be widespread with statistically significant differences (P < .05) in 48 out of 86 Brodmann areas. There were more statistically significant differences in the left hemisphere Brodmann areas (36 out of 43) than the number of Brodmann areas with statistical significance in the right hemisphere (12 out of 43). The theta frequency band had more statistically significant differences than other frequency bands.

Table 3 shows the results of paired t-tests in LORETA current density in the eyes open condition between socks off and socks on. The effects appeared to be widespread with statistically significant differences (P < .05) in 35 out of 86 Brodmann areas. There were more statistically significant differences in the left hemisphere.

Brodmann areas (22 out of 43) than the number of Brodmann areas with statistical significance in the right hemisphere (13 out of 43). The theta frequency band had more statistically significant differences than other frequency bands.

Figure 3 shows paired t-test (P < .0.001) results in the comparison of cortical current densities between standard socks versus Superneuro VTT enhanced socks in the eyes closed condition. Bilateral significant differences were present with left hemisphere differences more prominent than right hemisphere. The bilateral frontal lobes, including the sensory motor strip on the dorsal surface as well as the medial wall of the somatosensory projection regions of the foot (Homunculus) from 2 Hz to 7 Hz.

Figure 4 shows paired t-test (P < .0.001) results in the comparison of cortical current densities between standard socks versus Superneuro VTT socks in the eyes open condition. Bilateral significant differences were present with left hemisphere differences more prominent than right hemisphere. The bilateral frontal lobes, including the sensory motor strip on the dorsal surface as well as the medial wall of the somatosensory projection regions of the foot (Homunculus). Significant differences were also present in the left Para-hippocampal gyms and the left inferior frontal lobes from 2 Hz to 7 Hz.

Safety

Patients reported no adverse skin reactions, serious adverse events while wearing the socks embedded with the haptic vibrotactile trigger technology.

Discussion

The results of this study showed that the EEG auto and cross-spectrum is effected when the Superneuro VTT enhanced socks

FFT Coherence Group Paired t-Test (P-Value)

Intrahemispheric: LEFT

	DELTA	THETA	ALPHA	BETA
FP1 F3	0.002	0.134	0.358	0.625
FP1 C3	0.018	0.141	0.851	0.620
FP1 P3	0.240	0.015	0.040	0.317
FP1 O1	0.350	0.399	0.186	0.164
FP1 F7	0.022	0.347	0.617	0.477
FP1 T3	0.001	0.039	0.859	0.766
FP1 T5	0.265	0.788	0.100	0.244
F3 C3	0.012	0.001	0.585	0.423
F3 P3	0.425	0.142	0.044	0.399
F3 O1	0.788	0.448	0.102	0.392
F3 F7	0.958	0.038	0.130	0.138
F3 T3	0.030	0.030	0.080	0.245
F3 T5	0.205	0.229	0.078	0.494
C3 P3	0.731	0.201	0.889	0.414
C3 O1	0.959	0.944	0.110	0.994
C3 F7	0.392	0.051	0.302	0.366
C3 T3	0.082	0.042	0.551	0.699
C3 T5	0.075	0.189	0.418	0.662
P3 O1	0.014	0.047	0.510	0.080
P3 F7	0.118	0.391	0.034	0.216
P3 T3	0.254	0.443	0.436	0.932
P3 T5	0.508	0.060	0.289	0.260
O1 F7	0.379	0.601	0.280	0.272
O1 T3	0.871	0.847	0.898	0.779
O1 T5	0.069	0.073	0.333	0.158
F7 T3	0.888	0.098	0.239	0.144
F7 T5	0.976	0.841	0.125	0.347
T3 T5	0.010	0.160	0.599	0.449

Intrahemispheric: RIGHT

	DELTA	THETA	ALPHA	BETA
FP2 F4	0.002	0.027	0.856	0.698
FP2 C4	0.002	0.463	0.691	0.264
FP2 P4	0.337	0.109	0.035	0.011
FP2 O2	0.827	0.624	0.742	0.547
FP2 F8	0.253	0.221	0.380	0.738
FP2 T4	0.010	0.041	0.095	0.159
FP2 T6	0.708	0.944	0.928	0.330
F4 C4	0.046	0.569	0.447	0.119
F4 P4	0.095	0.077	0.021	0.028
F4 O2	0.956	0.482	0.394	0.480
F4 F8	0.112	0.150	0.500	0.900
F4 T4	0.004	0.019	0.082	0.132
F4 T6	0.427	0.675	0.326	0.318
C4 P4	0.250	0.027	0.127	0.884
C4 O2	0.661	0.037	0.026	0.318
C4 F8	0.003	0.371	0.882	0.270
C4 T4	0.003	0.003	0.491	0.251
C4 T6	0.013	0.041	0.435	0.729
P4 O2	0.066	0.160	0.815	0.192
P4 F8	0.839	0.437	0.031	0.080
P4 T4	0.033	0.012	0.024	0.009
P4 T6	0.038	0.038	0.173	0.085
O2 F8	0.500	0.631	0.809	0.338
O2 T4	0.342	0.264	0.960	0.470
O2 T6	0.108	0.098	0.730	0.867
F8 T4	0.050	0.004	0.069	0.108
F8 T6	0.103	0.585	0.921	0.143
T4 T6	0.020	0.015	0.037	0.001

Interhemispheric: HOMOLOGOUS PAIRS

	DELTA	THETA	ALPHA	BETA
FP1 FP2	0.393	0.426	0.098	0.209
C3 C4	0.044	0.235	0.415	0.424
O1 O2	0.355	0.048	0.245	0.943
T3 T4	0.018	0.501	0.571	0.693

	DELTA	THETA	ALPHA	BETA
F3 F4	0.016	0.222	0.621	0.518
P3 P4	0.025	0.010	0.481	0.022
F7 F8	0.366	0.783	0.666	0.292
T5 T6	0.426	0.229	0.953	0.502

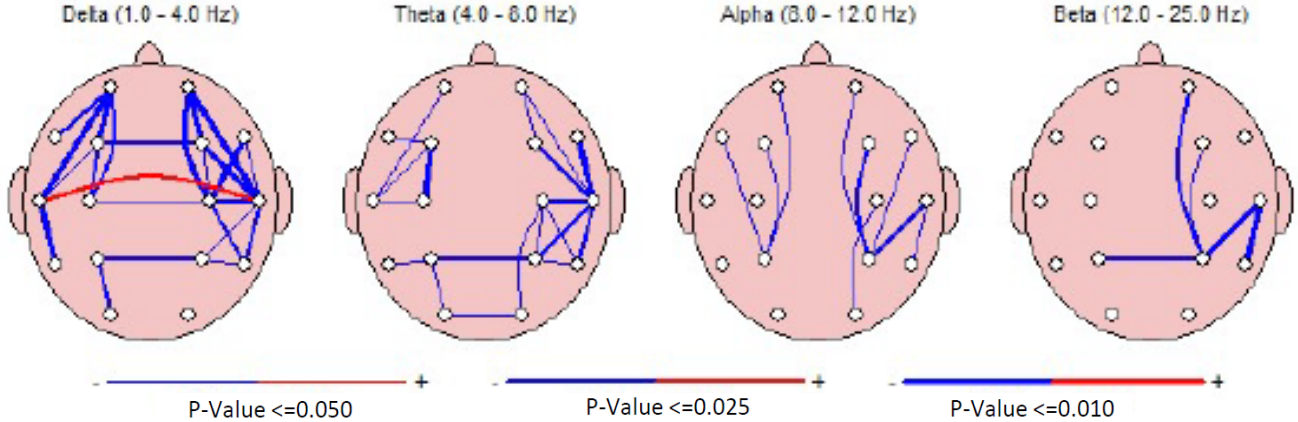

Figure 1: Paired t-tests in surface EEG coherence between socks off vs socks on in the eyes closed condition.

FFT Coherence Group Paired t-Test (P-Value)

Intrahemispheric: LEFT

	DELTA	THETA	ALPHA	BETA
FP1 F3	0.010	0.030	0.200	0.810
FP1 C3	0.219	0.712	0.710	0.682
FP1 P3	0.246	0.911	0.705	0.722
FP1 O1	0.715	0.724	0.905	0.030
FP1 F7	0.351	0.155	0.380	0.695
FP1 T3	0.275	0.992	0.976	0.724
FP1 T5	0.151	0.755	0.704	0.075
F3 C3	0.016	0.020	0.784	0.666
F3 P3	0.091	0.044	0.269	0.148
F3 O1	0.855	0.051	0.424	0.040
F3 F7	0.616	0.007	0.016	0.844
F3 T3	0.054	0.190	0.567	0.774
F3 T5	0.493	0.084	0.752	0.024
C3 P3	0.277	0.174	0.261	0.390
C3 O1	0.927	0.122	0.354	0.102
C3 F7	0.786	0.272	0.262	0.461
C3 T3	0.277	0.840	0.650	0.991
C3 T5	0.546	0.105	0.317	0.129
P3 O1	0.070	0.011	0.228	0.016
P3 F7	0.183	0.209	0.239	0.226
P3 T3	0.793	0.427	0.943	0.936
P3 T5	0.218	0.024	0.102	0.029
O1 F7	0.777	0.871	0.680	0.033
O1 T3	0.247	0.703	0.743	0.753
O1 T5	0.199	0.103	0.289	0.144
F7 T3	0.631	0.999	0.844	0.234
F7 T5	0.425	0.499	0.278	0.048
T3 T5	0.014	0.510	0.823	0.462

Intrahemispheric: RIGHT

	DELTA	THETA	ALPHA	BETA
FP2 F4	0.171	0.157	0.710	0.111
FP2 C4	0.133	0.155	0.742	0.140
FP2 P4	0.303	0.035	0.696	0.121
FP2 O2	0.956	0.619	0.824	0.162
FP2 F8	0.593	0.779	0.806	0.238
FP2 T4	0.003	0.004	0.416	0.074
FP2 T6	0.858	0.195	0.551	0.080
F4 C4	0.084	0.327	0.369	0.329
F4 P4	0.908	0.051	0.208	0.024
F4 O2	0.784	0.115	0.353	0.222
F4 F8	0.884	0.947	0.764	0.291
F4 T4	0.014	0.028	0.631	0.123
F4 T6	0.892	0.156	0.746	0.071
C4 P4	0.822	0.256	0.160	0.333
C4 O2	0.817	0.715	0.857	0.241
C4 F8	0.026	0.153	0.577	0.139
C4 T4	0.000	0.028	0.456	0.401
C4 T6	0.005	0.993	0.202	0.770
P4 O2	0.112	0.169	0.510	0.116
P4 F8	0.878	0.166	0.547	0.277
P4 T4	0.032	0.107	0.251	0.038
P4 T6	0.700	0.535	0.432	0.101
O2 F8	0.539	0.126	0.941	0.075
O2 T4	0.389	0.183	0.532	0.052
O2 T6	0.290	0.078	0.404	0.841
F8 T4	0.012	0.007	0.469	0.333
F8 T6	0.504	0.113	0.389	0.114
T4 T6	0.000	0.016	0.387	0.014

Interhemispheric: HOMOLOGOUS PAIRS

	DELTA	THETA	ALPHA	BETA
FP1 FP2	0.238	0.595	0.883	0.090
C3 C4	0.017	0.516	0.956	0.188
O1 O2	0.302	0.035	0.693	0.027
T3 T4	0.644	0.821	0.839	0.315

	DELTA	THETA	ALPHA	BETA
F3 F4	0.052	0.014	0.088	0.398
P3 P4	0.117	0.023	0.435	0.004
F7 F8	0.444	0.939	0.491	0.522
T5 T6	0.081	0.099	0.693	0.094

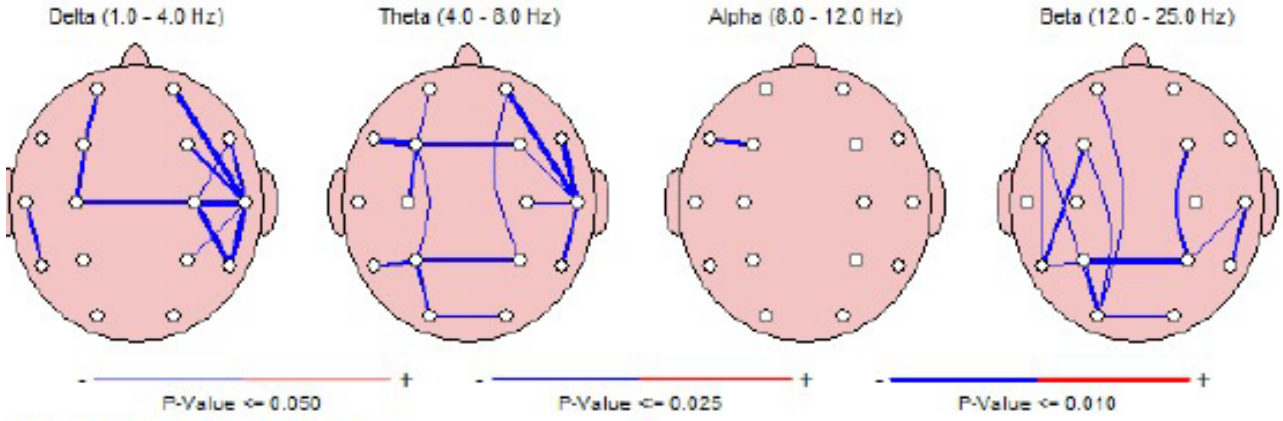

Figure 2: Paired t-tests in surface EEG coherence between socks off vs socks on in the eyes open condition.

Group Paired T-TEST RESULTs: EC_Loreta Absolute Power_noVoxx vs Voxx_n=60 Subjects																	
LEFT	DELTA	THETA	ALPHA1	ALPHA2	BETA1	BETA2	BETA3	HI-BETA	RIGHT	DELTA	THETA	ALPHA1	ALPHA2	BETA1	BETA2	BETA3	HI-BETA
BA_1L	0.0091	0.0068	0.2520	0.9683	0.8969	0.5452	0.4724	0.6195	BA_1R	0.6676	0.4232	0.5150	0.6277	0.7651	0.5073	0.4322	0.5111
BA_2L	0.0072	0.0345	0.4136	0.6813	0.5585	0.3207	0.2846	0.4908	BA_2R	0.8443	0.6485	0.6381	0.4071	0.5712	0.4329	0.2906	0.3416
BA_3L	0.0048	0.0246	0.3873	0.7364	0.5895	0.3414	0.3028	0.5003	BA_3R	0.8712	0.6608	0.6632	0.3999	0.5564	0.4159	0.2841	0.3402
BA_4L	0.0549	0.0063	0.7224	0.4776	0.7284	0.3715	0.3555	0.4147	BA_4R	0.3642	0.2016	0.2973	0.9828	0.9371	0.7788	0.7497	0.8860
BA_5L	0.9235	0.5765	0.8976	0.1642	0.5638	0.4701	0.3810	0.6696	BA_5R	0.9862	0.5825	0.9581	0.1631	0.5011	0.3988	0.3217	0.5716
BA_6L	0.2556	0.4902	0.8433	0.2022	0.3498	0.2402	0.2016	0.4114	BA_6R	0.7898	0.9780	0.6941	0.1638	0.2859	0.2996	0.2001	0.3279
BA_7L	0.9216	0.6031	0.9725	0.1960	0.6279	0.5950	0.5319	0.9330	BA_7R	0.8932	0.6066	0.9795	0.2013	0.6259	0.5916	0.5359	0.9334
BA_8L	0.0026	0.0007	0.4090	0.6143	0.5821	0.2953	0.3263	0.4245	BA_8R	0.3995	0.6573	0.9038	0.4959	0.4760	0.4405	0.3699	0.3865
BA_9L	0.0025	0.0006	0.4403	0.5852	0.5766	0.2933	0.3256	0.4201	BA_9R	0.3875	0.6649	0.9168	0.4965	0.4667	0.4401	0.3704	0.3864
BA_10L	0.0894	0.0729	0.3915	0.2252	0.3932	0.2867	0.2010	0.2663	BA_10R	0.1691	0.2811	0.4385	0.1370	0.2257	0.2617	0.2708	0.3775
BA_11L	0.0551	0.0568	0.3042	0.1133	0.2070	0.2186	0.1893	0.3266	BA_11R	0.0470	0.0603	0.3049	0.1021	0.1909	0.2167	0.1984	0.3414
BA_13L	0.1019	0.0359	0.5031	0.7753	0.6183	0.7994	0.6840	0.6131	BA_13R	0.1665	0.1794	0.2271	0.9009	0.9409	0.8879	0.8143	0.8685
BA_17L	0.0842	0.0355	0.0589	0.3766	0.3429	0.8939	0.7262	0.9601	BA_17R	0.0918	0.0372	0.0626	0.3586	0.3662	0.9395	0.7072	0.9763
BA_18L	0.0517	0.0308	0.0411	0.5083	0.1878	0.6255	0.9638	0.6298	BA_18R	0.1404	0.0475	0.0720	0.3465	0.4452	0.9438	0.7231	0.8457
BA_19L	0.0412	0.0451	0.0302	0.4584	0.1407	0.4858	0.7388	0.4436	BA_19R	0.2014	0.1028	0.0402	0.5082	0.3508	0.7749	0.9828	0.5011
BA_20L	0.0864	0.0324	0.2758	0.6705	0.2322	0.7919	0.9921	0.9942	BA_20R	0.2190	0.1339	0.0858	0.6900	0.4267	0.7947	0.9339	0.9931
BA_21L	0.0944	0.0409	0.3714	0.7343	0.2700	0.8335	0.9445	0.9541	BA_21R	0.2536	0.1761	0.1360	0.6741	0.4859	0.7981	0.9248	0.9385
BA_22L	0.1018	0.0421	0.1299	0.6930	0.1890	0.4411	0.3532	0.2800	BA_22R	0.2822	0.0359	0.0684	0.2274	0.0781	0.3108	0.3884	0.4105
BA_23L	0.0966	0.0509	0.0452	0.3621	0.3664	0.8440	0.7171	0.9937	BA_23R	0.1063	0.0606	0.0500	0.3411	0.4060	0.9118	0.7019	0.9865
BA_24L	0.0500	0.0273	0.4855	0.0830	0.3046	0.3099	0.2651	0.4329	BA_24R	0.0500	0.0282	0.4919	0.0805	0.3017	0.3112	0.2688	0.4365
BA_25L	0.0460	0.0255	0.4386	0.1053	0.2981	0.2835	0.2481	0.4016	BA_25R	0.0445	0.0384	0.5531	0.0944	0.3133	0.3216	0.3031	0.4449
BA_27L	0.0402	0.0035	0.0694	0.4698	0.2040	0.7197	0.5886	0.6544	BA_27R	0.0514	0.0122	0.0143	0.2475	0.3827	0.8101	0.5870	0.6083
BA_28L	0.0799	0.0260	0.1481	0.6575	0.2526	0.8554	0.8378	0.8010	BA_28R	0.1342	0.1486	0.0950	0.9488	0.6299	0.9910	0.8584	0.8049
BA_29L	0.0533	0.0165	0.0802	0.8241	0.3276	0.6217	0.5786	0.5814	BA_29R	0.2078	0.1270	0.1917	0.8757	0.4826	0.9963	0.9805	0.8022
BA_30L	0.0289	0.0111	0.0322	0.4541	0.2708	0.6443	0.6002	0.7712	BA_30R	0.0933	0.0189	0.0182	0.2888	0.4456	0.9223	0.6081	0.7436
BA_31L	0.1113	0.0946	0.0391	0.3506	0.4042	0.7449	0.7068	0.9740	BA_31R	0.1324	0.1581	0.0502	0.3089	0.5315	0.9486	0.6801	0.9149
BA_32L	0.0995	0.1307	0.3118	0.1307	0.2449	0.2671	0.2027	0.3708	BA_32R	0.0996	0.1436	0.3210	0.1166	0.2104	0.2483	0.1959	0.3878
BA_33L	0.1352	0.1737	0.4701	0.7354	0.6525	0.3309	0.3729	0.4716	BA_33R	0.3068	0.3829	0.4521	0.4100	0.5028	0.2870	0.3044	0.4302
BA_34L	0.0827	0.0275	0.2416	0.7491	0.3639	0.9956	0.7145	0.6856	BA_34R	0.1525	0.1795	0.1969	0.9966	0.8154	0.9121	0.7855	0.7709
BA_35L	0.0639	0.0127	0.0849	0.7367	0.2227	0.8389	0.8033	0.8021	BA_35R	0.0639	0.0345	0.0165	0.4236	0.3646	0.8280	0.7681	0.7007
BA_36L	0.0813	0.0281	0.1886	0.6251	0.2632	0.8711	0.8372	0.8072	BA_36R	0.1659	0.1862	0.1382	0.9951	0.6684	0.9945	0.8813	0.8305
BA_37L	0.0092	0.0450	0.0732	0.4213	0.1486	0.4780	0.5573	0.4776	BA_37R	0.2462	0.1150	0.0254	0.6817	0.2327	0.3259	0.6465	0.5161
BA_38L	0.0859	0.0337	0.3647	0.7523	0.3514	0.9852	0.7471	0.7587	BA_38R	0.2579	0.2598	0.2688	0.9828	0.7638	0.9824	0.8822	0.8616
BA_39L	0.0477	0.0663	0.0568	0.4134	0.2112	0.6522	0.9963	0.6001	BA_39R	0.1701	0.1518	0.0415	0.6296	0.3001	0.6926	0.9144	0.4524
BA_40L	0.0447	0.0104	0.1503	0.8100	0.5635	0.9650	0.9936	0.9779	BA_40R	0.3747	0.1426	0.2750	0.8902	0.6654	0.8544	0.8644	0.9590
BA_41L	0.0801	0.0274	0.0975	0.7372	0.2420	0.5053	0.4252	0.3850	BA_41R	0.3551	0.1087	0.2410	0.8273	0.6201	0.9369	0.9188	0.8567
BA_42L	0.0933	0.0330	0.1374	0.7107	0.2656	0.5554	0.4664	0.4054	BA_42R	0.3085	0.0464	0.1117	0.3611	0.1602	0.5363	0.5404	0.5281
BA_43L	0.0760	0.0221	0.1629	0.7557	0.4107	0.7729	0.7271	0.6862	BA_43R	0.3695	0.0801	0.1838	0.6059	0.3682	0.8448	0.8076	0.7587
BA_44L	0.0720	0.0215	0.7279	0.7492	0.8061	0.5972	0.4104	0.4600	BA_44R	0.2516	0.3003	0.6236	0.6829	0.7969	0.6662	0.5714	0.5935
BA_45L	0.0731	0.0220	0.6682	0.8028	0.7471	0.6316	0.4321	0.4744	BA_45R	0.2400	0.2877	0.5472	0.7677	0.8576	0.7120	0.6052	0.6303
BA_46L	0.0068	0.0011	0.4093	0.7755	0.7842	0.3892	0.3761	0.4342	BA_46R	0.3109	0.4519	0.8119	0.6379	0.6498	0.5553	0.4850	0.4880
BA_47L	0.0831	0.0315	0.5945	0.9085	0.5917	0.7766	0.5401	0.5789	BA_47R	0.2344	0.2643	0.4375	0.8357	0.9651	0.8050	0.6972	0.7128
AmygL	0.0822	0.0279	0.1816	0.6749	0.2744	0.8834	0.8133	0.7815	AmygR	0.1486	0.1661	0.1183	0.9600	0.6716	0.9924	0.8501	0.8078
HippL	0.0797	0.0247	0.1364	0.7400	0.2642	0.8711	0.8067	0.7747	HippR	0.1163	0.1264	0.0750	0.8242	0.6357	0.9906	0.8081	0.7645

Table 2: Paired t-tests in LORETA current density between socks off vs socks on in the eyes closed condition.

Group Paired T-TEST RESULTs: EO_Loreta Absolute Power_noVoxx vs Voxx_n=60 Subjects																	
LEFT	DELTA	THETA	ALPHA1	ALPHA2	BETA1	BETA2	BETA3	HI-BETA	RIGHT	DELTA	THETA	ALPHA1	ALPHA2	BETA1	BETA2	BETA3	HI-BETA
BA_1L	0.4663	0.1039	0.2409	0.2771	0.3075	0.3273	0.3735	0.5930	BA_1R	0.0704	0.5317	0.4592	0.5135	0.8274	0.6577	0.8733	0.7781
BA_2L	0.6434	0.1692	0.3803	0.4135	0.3711	0.5906	0.6211	0.7509	BA_2R	0.1829	0.6356	0.4527	0.6814	0.7995	0.6593	0.9138	0.8302
BA_3L	0.6238	0.1632	0.3642	0.4074	0.3706	0.5469	0.5864	0.7285	BA_3R	0.1703	0.6577	0.4854	0.7179	0.7562	0.6873	0.8853	0.8367
BA_4L	0.2707	0.0676	0.2688	0.1620	0.2325	0.3280	0.4774	0.4523	BA_4R	0.1385	0.3185	0.3631	0.2569	0.7217	0.4682	0.8942	0.9541
BA_5L	0.7268	0.6729	0.1962	0.2753	0.2767	0.2945	0.0753	0.0715	BA_5R	0.6751	0.6200	0.1790	0.2709	0.2593	0.3339	0.0745	0.0829
BA_6L	0.8136	0.3446	0.5341	0.4506	0.5687	0.7066	0.7440	0.7839	BA_6R	0.1317	0.6405	0.4425	0.6307	0.8578	0.6841	0.9652	0.9864
BA_7L	0.7325	0.6322	0.1851	0.2741	0.2342	0.2812	0.0398	0.0272	BA_7R	0.7217	0.6296	0.1850	0.2748	0.2326	0.2880	0.0393	0.0270
BA_8L	0.2270	0.0268	0.1253	0.1003	0.1968	0.4314	0.7542	0.7415	BA_8R	0.1120	0.3504	0.5028	0.7796	0.7258	0.9210	0.7955	0.9328
BA_9L	0.2204	0.0263	0.1298	0.0994	0.1968	0.4277	0.7489	0.7181	BA_9R	0.1117	0.3545	0.5206	0.7994	0.7205	0.9344	0.7869	0.9395
BA_10L	0.1535	0.0667	0.4818	0.2924	0.4865	0.5220	0.6399	0.6297	BA_10R	0.2555	0.1841	0.7732	0.5351	0.8054	0.6774	0.5773	0.8664
BA_11L	0.1515	0.0634	0.5424	0.3866	0.6047	0.6218	0.9183	0.8781	BA_11R	0.1486	0.0600	0.5701	0.4188	0.6542	0.6547	0.9922	0.9143
BA_13L	0.2011	0.0559	0.1677	0.0720	0.1396	0.2250	0.3025	0.4347	BA_13R	0.5262	0.3187	0.4953	0.2325	0.6630	0.6913	0.7786	0.9149
BA_17L	0.0546	0.0075	0.0868	0.1536	0.1137	0.2961	0.0975	0.0757	BA_17R	0.0598	0.0087	0.0962	0.1670	0.1177	0.3130	0.0973	0.0742
BA_18L	0.0810	0.0060	0.0373	0.0614	0.0840	0.1969	0.0815	0.0810	BA_18R	0.0901	0.0150	0.0766	0.1431	0.0944	0.3175	0.1100	0.0747
BA_19L	0.1195	0.0092	0.0378	0.0443	0.0662	0.1587	0.0507	0.0732	BA_19R	0.1706	0.0403	0.0554	0.0950	0.0687	0.2342	0.0992	0.0838
BA_20L	0.2216	0.0836	0.1377	0.0645	0.1339	0.2006	0.2724	0.5036	BA_20R	0.6476	0.4074	0.3603	0.1762	0.6293	0.6005	0.8701	0.8146
BA_21L	0.2224	0.0895	0.1546	0.0703	0.1461	0.2064	0.2800	0.4899	BA_21R	0.7160	0.4353	0.4111	0.2042	0.6506	0.5714	0.8380	0.8067
BA_22L	0.2269	0.0520	0.1243	0.0972	0.1764	0.1001	0.1334	0.3804	BA_22R	0.2296	0.0638	0.0672	0.0192	0.1482	0.1545	0.7291	0.6268
BA_23L	0.0666	0.0089	0.1016	0.1797	0.1111	0.2939	0.0861	0.0791	BA_23R	0.0816	0.0128	0.1143	0.1971	0.1187	0.3167	0.0854	0.0766
BA_24L	0.1621	0.0540	0.3240	0.2428	0.5165	0.5696	0.9116	0.9100	BA_24R	0.1638	0.0549	0.3264	0.2470	0.5278	0.5771	0.9274	0.9155
BA_25L	0.1439	0.0503	0.3602	0.2634	0.5277	0.5753	0.9014	0.9091	BA_25R	0.1546	0.0571	0.3749	0.3005	0.6452	0.6495	0.9491	0.9509
BA_27L	0.1113	0.0060	0.0567	0.0457	0.0694	0.2470	0.2939	0.4578	BA_27R	0.2564	0.0225	0.1638	0.2252	0.0867	0.3875	0.4744	0.5687
BA_28L	0.1920	0.0649	0.1236	0.0520	0.1280	0.2348	0.3472	0.5641	BA_28R	0.6889	0.4157	0.4501	0.2851	0.7827	0.7569	0.8400	0.8595
BA_29L	0.1485	0.0261	0.1167	0.1470	0.2326	0.1170	0.1376	0.3979	BA_29R	0.0202	0.0415	0.1050	0.1058	0.3086	0.3541	0.5775	0.5191
BA_30L	0.0513	0.0027	0.0727	0.1250	0.0747	0.2595	0.1320	0.1695	BA_30R	0.1032	0.0165	0.1486	0.2411	0.1123	0.3757	0.1160	0.1295
BA_31L	0.0815	0.0097	0.1066	0.1962	0.0967	0.2682	0.0728	0.0840	BA_31R	0.1303	0.0317	0.1376	0.2357	0.1196	0.3377	0.0752	0.0795
BA_32L	0.1853	0.0711	0.5292	0.3653	0.4791	0.5261	0.7175	0.6982	BA_32R	0.1800	0.0623	0.5256	0.3693	0.4770	0.5248	0.8107	0.7320
BA_33L	0.0042	0.0005	0.0251	0.0181	0.1451	0.4167	0.7581	0.7814	BA_33R	0.0064	0.0062	0.0366	0.0366	0.1610	0.4148	0.7162	0.7829
BA_34L	0.1864	0.0623	0.1321	0.0553	0.1398	0.2427	0.3767	0.5574	BA_34R	0.6533	0.4009	0.4794	0.3172	0.8570	0.7657	0.8134	0.8675
BA_35L	0.1947	0.0417	0.0766	0.0410	0.0920	0.2238	0.3072	0.5317	BA_35R	0.4456	0.1055	0.1758	0.1735	0.2233	0.5052	0.9071	0.8046
BA_36L	0.1912	0.0682	0.1318	0.0564	0.1358	0.2349	0.3447	0.5655	BA_36R	0.7196	0.4860	0.5231	0.3348	0.8822	0.7810	0.8204	0.8578
BA_37L	0.3093	0.0395	0.0758	0.0703	0.0698	0.1239	0.0521	0.1682	BA_37R	0.2600	0.0674	0.0499	0.0661	0.0551	0.1676	0.1143	0.1891
BA_38L	0.1950	0.0752	0.1541	0.0696	0.1574	0.2407	0.3416	0.5548	BA_38R	0.7613	0.5707	0.6358	0.4196	0.9823	0.7745	0.7964	0.8468
BA_39L	0.2302	0.0264	0.0498	0.0406	0.0599	0.1584	0.0556	0.0755	BA_39R	0.2434	0.0769	0.0642	0.1095	0.0819	0.2295	0.0880	0.0731
BA_40L	0.2547	0.0423	0.1487	0.1679	0.2482	0.1673	0.2035	0.4601	BA_40R	0.0375	0.1986	0.2389	0.1511	0.6981	0.4386	0.9525	0.6748
BA_41L	0.1759	0.0310	0.1198	0.1225	0.2080	0.1048	0.1311	0.3849	BA_41R	0.0868	0.2946	0.3282	0.1702	0.6309	0.4322	0.9718	0.8404
BA_42L	0.2163	0.0390	0.1370	0.1223	0.2056	0.1129	0.1443	0.3927	BA_42R	0.1485	0.0767	0.1044	0.0332	0.2577	0.2079	0.7941	0.6390
BA_43L	0.2479	0.0399	0.1544	0.1508	0.2338	0.1405	0.1720	0.4198	BA_43R	0.0982	0.1566	0.1871	0.0786	0.4820	0.3011	0.9122	0.6778
BA_44L	0.1669	0.0482	0.1638	0.0762	0.1846	0.2794	0.4202	0.5550	BA_44R	0.4107	0.2990	0.4690	0.3521	0.9018	0.7127	0.7735	0.8339
BA_45L	0.1701	0.0505	0.1579	0.0729	0.1758	0.2709	0.4050	0.5459	BA_45R	0.4557	0.3171	0.4597	0.3390	0.8639	0.7051	0.7824	0.8318
BA_46L	0.0769	0.0050	0.0600	0.0497	0.1720	0.3712	0.7035	0.7640	BA_46R	0.1894	0.2525	0.4616	0.4949	0.8859	0.8501	0.7846	0.8737
BA_47L	0.1837	0.0657	0.1683	0.0778	0.1802	0.2698	0.3937	0.5731	BA_47R	0.6152	0.4297	0.5742	0.4045	0.9466	0.7613	0.7796	0.8579
AmygL	0.1930	0.0668	0.1296	0.0547	0.1324	0.2358	0.3464	0.5546	AmygR	0.7139	0.4407	0.4840	0.3078	0.8234	0.7680	0.8290	0.8605
HippL	0.1930	0.0616	0.1188	0.0498	0.1239	0.2367	0.3473	0.5536	HippR	0.6652	0.3534	0.3944	0.2608	0.7039	0.7400	0.8569	0.8620

Table 3: Paired t-tests in LORETA current density between socks off vs socks on in the eyes open condition.

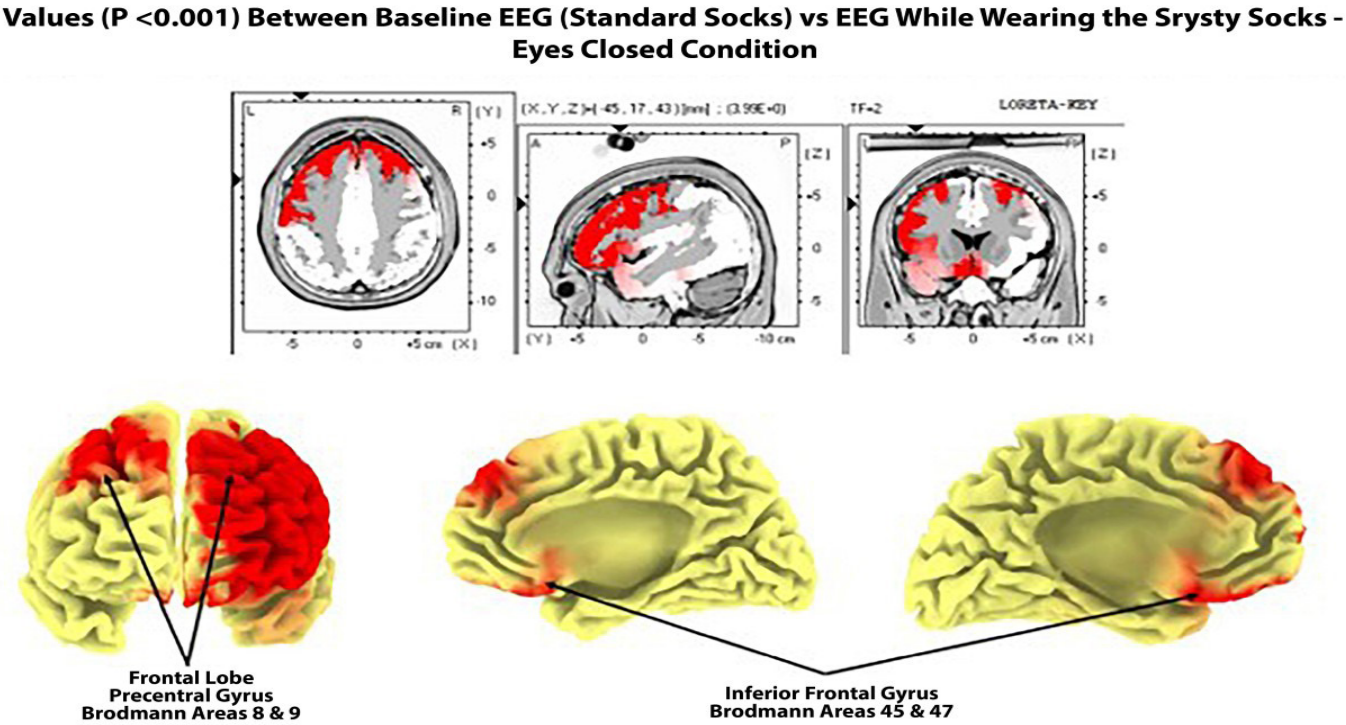

Figure 3: Paired t-test (P<0.001) differences in current density between standard socks versus Superneuro VTT enhanced socks in the eyes closed condition.

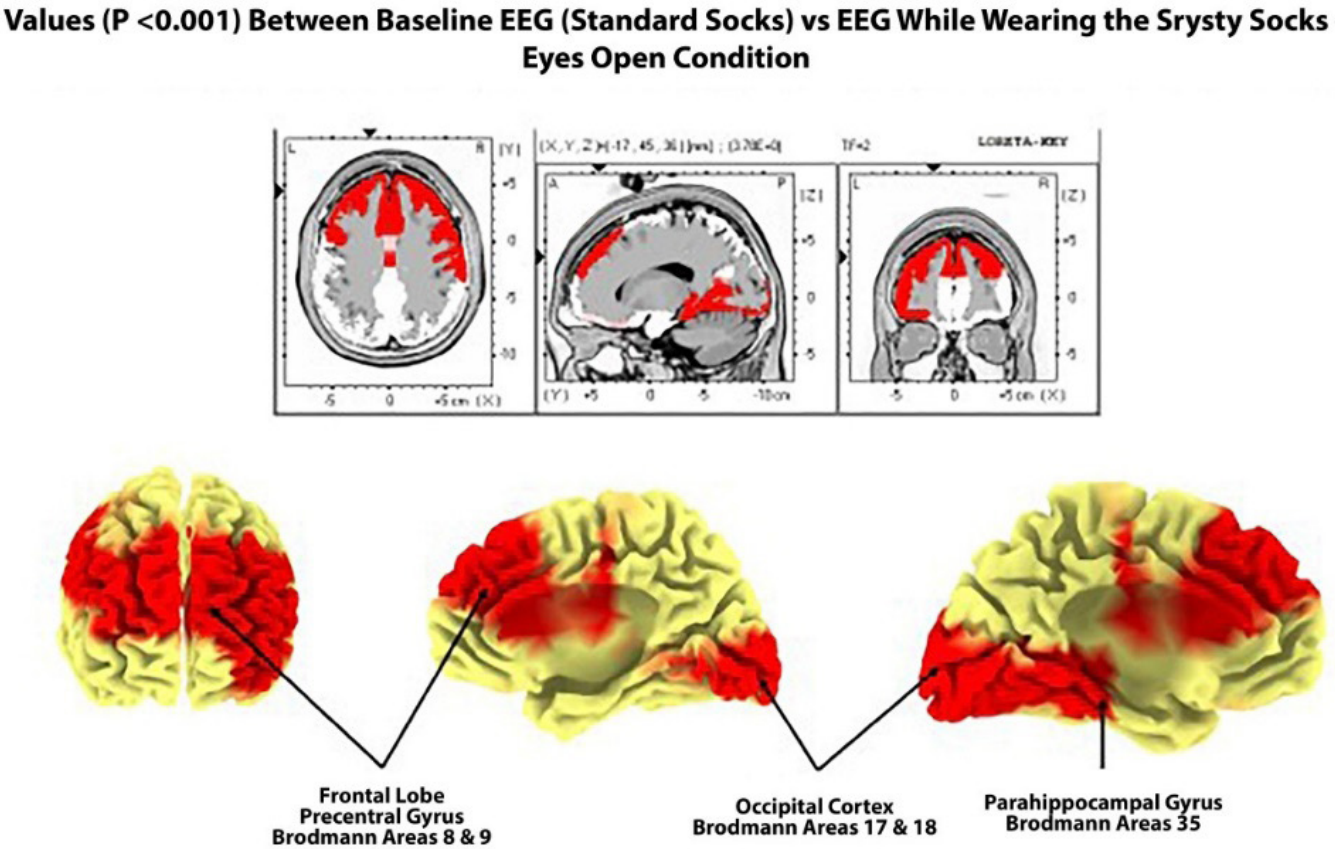

Figure 4: Paired t-test (P<0.001) differences in current density between standard socks versus Superneuro VTT enhanced socks in the eyes open condition.

are placed on a person's feet as compared to a random sample of regularly worn socks. Fifty nine out of 60 subjects exhibited statistically significant changes in surface auto and cross-spectrum. Sixty out of sixty of the subjects exhibited statistically significant changes in the EEG source current density.

There was generally an increase in EEG absolute power in the delta and theta frequency bands, especially in the left hemisphere and a decrease in power in the higher frequency bands, especially in the right hemisphere with Superneuro VTT enhanced socks on vs Superneuro VTT enhanced socks off. EEG coherence primarily decreased with Superneuro VTT socks on vs regular socks in all frequency bands and in both hemispheres. Decreased coherence indicates increased differentiation and increased complexity in brain networks.

Validation of the effects of the somatosensory foot stimulation on the central nervous system was further provided by the finding that LORETA current density consistently increased in the foot projection areas on the medial surface of the somatosensory cortex. Bilateral frontal lobe Brodmann areas exhibited the largest t-test differences (99.9%) in the lower frequency bands (e.g., delta and theta) and especially in left hemisphere Brodmann areas. The effects of Superneuro VTT enhanced socks on the electrical energies of the brain were evident especially in left frontal and left temporal, left anterior cingulate and left parahippocampal gyrus.

The exact mechanisms of action of the Superneuro VTT enhanced sock foot pattern on the somatosensory system are currently unknown. At least three hypotheses are: 1- The process of changing socks effects the EEG spectrum, 2- Dishabituation occurs because of the novelty of a sequence of edges that stimulate the foot and, 3- Both hypotheses 1 and 2 contributed to the EEG changes.

During EEG readings where the subjects' eyes were open or closed, Superneuro VTT enhanced socks activated 35 out of 86 BA (left and right hemispheres combined) and 48 out of 86 BA (left and right hemispheres combined), respectively. Among BA that were activated by Superneuro VTT enhanced socks in a statistically significant manner, 10 out of 12 overlapped with the review: 9,11, 24, 39, 40, 44- 47. When compared to standard socks, activation in the medial somatosensory cortex, parts of the occipital lobe, and bilateral frontal lobes were statistically higher while wearing Superneuro VTT enhanced socks ($p<0.001$). The associated BA here overlapped with the data from the review as well, with overlap found in BA 9, 45, and 47 [20]. Thus, it appears that the brain activation observed following tactile stimulation of somatosensory activity intersects strongly with brain activation in response to noxious stimuli, implying a similar relationship to the neuromatrix. Other studies have noted that the brain regions activated as part of a neurosignature response to pain are also activated during non-noxious stimuli [21,23], which suggests that the perception of pain resulting from cortical response is context dependent. The context dependent nature of an individual's response to pain is also reflected in studies indicating that the intensity of response is proportional to the perceived strength of the stimulus [24]. These findings may also explain the numerous regions and BA that are associated with the perception of pain, which may be due to the high degree of variability in pain perception between individuals [21,25] The findings presented here strongly suggest that Superneuro VTT enhanced socks could have an influence on the subject's pain management and modulation. Taken together, results reported here from this IRB-approved study lends further credence to the hypothesis that disruption or modulation of pain inputs originating from an internal source, outside an acute pain event, could be a viable treatment for those experiencing chronic pain [20,25].

Alternative treatment options that have minimal adverse effects as compared to conventional systemic analgesics are needed in order to provide better options to clinicians. A better understanding of the neuromatrix and identifying novel, non-pharmacological treatments will add important safe and effective options to a clinician's pain management approach to patient care [26-31].

Conclusion

Study results indicate that non-invasive, non-pharmacological products embedded with haptic vibrotactile trigger technology may be useful in disrupting the neuromatrix of pain and have an impact on patient's pain levels. The results support further research into the use of this haptic vibrotactile trigger technology to evaluate if this technology has a positive impact on pain severity, pain interference, and quality of life and to be considered as a potentially beneficial pain management strategy and as part of a multi-modal treatment approach.

Acknowledgments

This IRB-approved study was funded by SRYSTY Holding CO., the distributors of the Superneuro VTT Enhanced Socks.

Disclosure

Robert Thatcher, PhD received compensation from SRYSTY Holding Co. for providing statistical analysis. Mark Debrincat, DC received compensation for his role as site Investigator. John Haddad, PhD received compensation for study interpretation. Baldeep Dhaliwal, MD was not compensated. Peter L Hurwitz was compensated for data review and study interpretation.

References

1. Finley CR, Chan DS, Garrison S, et al. What are the most common conditions in primary care? Systematic review. Can Fam Physician. 2018; 64: 832-840.
2. Volkow N, Benveniste H, McLellan AT. Use and misuse of opioids in chronic pain. Ann Rev Med. 2018; 69: 451-465.
3. Ambrose KR, Golightly YM. Physical exercise as non-pharmacological treatment of chronic pain: why and when. Best Pract Res Clin Rheumatol. 2015; 29: 120-130.
4. Ducic I, Mesbahi AN, Attinger CE, et al. The role of peripheral nerve surgery in the treatment of chronic pain associated with amputation stumps. Plastic Reconst Surgery. 2008; 121: 908-914.

5. De Williams AC, Eccleston C, Morley S. Psychological therapies for the management of chronic pain (excluding headache) in adults. Cochr Data Syst Rev. 2012; 11: 7407.
6. Sullivan MD, Howe CQ. Opioid therapy for chronic pain in the United States: promises and perils. PAIN. 2013; 154: 94-100.
7. Ballantyne JC, Sullivan MD. Intensity of chronic pain—the wrong metric. N Engl J Med. 2015; 373: 2098-2099.
8. Kaye AD, Cornett EM, Hart B, et al. Novel pharmacological nonopioid therapies in chronic pain. Curr Pain Head Rep. 2018; 22: 31.
9. Zhuo M. Neural mechanisms underlying anxiety–chronic pain interactions. Trends Neurosci. 2016; 39: 136-145.
10. Pohl M, Smith L. Chronic pain and addiction: challenging co-occurring disorders. J Psych Drugs. 2012; 44: 119-124.
11. Vowles KE, McEntee ML, Julnes PS, et al. Rates of opioid misuse, abuse, and addiction in chronic pain: a systematic review and data synthesis. Pain. 2015; 156: 569-576.
12. Volkow ND, McLellan AT. Opioid abuse in chronic pain—misconceptions and mitigation strategies. New Eng J Med. 2016; 374: 1253-1263.
13. Gao YJ, Ji RR. Targeting astrocyte signaling for chronic pain. Neurotherapeutics. 2010; 7: 482-493.
14. Cuomo A, Bimonte S, Forte CA, et al. Multimodal approaches and tailored therapies for pain management: the trolley analgesic model. J Pain Res. 2019; 12: 711-714.
15. Sharon L Kolasinski, Tuhina Neogi, Marc C Hochberg, et al. 2019 American College of Rheumatology/Arthritis Foundation Guideline for the Management of Osteoarthritis of the Hand, Hip, and Knee. Arthritis Care Res (Hoboken). 2020; 72: 149-162.
16. Chen J, Jin T, Zhang H. Nanotechnology in Chronic Pain Relief. Front Bioeng Biotechnol. 2020; 8: 682.
17. Melzack R. Pain and the neuromatrix in the brain. J Dent Educ. 2001; 65: 1378-1382.
18. Weiss T. Plasticity and cortical reorganization associated with pain. Z Psychol. 2016; 224: 71-79.
19. Diers M, Koeppe C, Diesch E, et al. Central processing of acute muscle pain in chronic low back pain patients: an EEG mapping study. J Clin Neurophysiol. 2007; 24: 76-83.
20. Derbyshire SWG. Exploring the pain "neuromatrix." Curr Rev Pain. 2000; 4: 467-477.
21. Mouraux A, Diukova A, Lee MC, et al. A multisensory investigation of the functional significance of the "pain matrix." Neuroimage. 2011; 54: 2237-2249.
22. Dahliwal J. VoxxLife Inc. Toronto CA. 2018.
23. Visser EJ, Davies S. Expanding Melzack's pain neuromatrix. The threat matrix: a super- system for managing polymodal threats. Pain Pract. 2010; 10: 163.
24. Khalsa PS. Biomechanics of musculoskeletal pain: dynamics of the neuromatrix. J Electromyogr Kinesiol. 2004; 14: 109-120.
25. Pergolizzi JV, Raffa RB, Taylor Jr R. Treating acute pain in light of the chronification of pain. Pain Manag Nurs. 2014; 15: 380-390.
26. Farkouh ME, Greenberg BP. An evidence-based review of the cardiovascular risks of nonsteroidal anti-inflammatory drugs. Am J Cardiol. 2009; 103: 1227-1237.
27. Harirforoosh S, Jamali F. Renal adverse effects of nonsteroidal anti-inflammatory drugs. Expert Opin Drug Saf. 2009; 8: 669-681.
28. John R, Herzenberg AM. Renal toxicity of therapeutic drugs. J Clin Pathol. 2009; 62: 505-515.
29. Lazzaroni M, Porro GB. Management of NSAID-induced gastrointestinal toxicity: focus on proton pump inhibitors. Drugs. 2009; 69: 51-69 .
30. Scarpignato C, Hunt RH. Nonsteroidal anti-inflammatory drug-related injury to the gastrointestinal tract: clinical picture, pathogenesis, and prevention. Gastroenterol Clin North Am. 2010; 39: 433-464.
31. Trelle S, Reichenbach S, Wandel S, et al. Cardiovascular safety of non-steroidal anti-inflammatory drugs: network meta-analysis. BMJ. 2011; 342: 7086.